3rd International Conference Advanced Mechanics: Structure, Materials, Tribology

Definition of the Feed Influence During the FSP Process of Steel Surfaces on Hardening by Alloying with WC-Co Tool Particles. Modeling and Experiment

Definition of the Feed Influence During the FSP Process of Steel Surfaces on Hardening by Alloying with WC-Co Tool Particles. Modeling and Experiment

Viktor P. Kuznetsov[a], Igor A. Vorontsov[b] and Andrei S. Skorobogatov[c]

Ural Federal University, 19 Mira St., 620062, Ekaterinburg, Russia

[a] Corresponding author: wpkuzn@mail.ru
[b] igor.vorontsov@urfu.ru
[c] ufo2log@gmail.com

Abstract. The article presents an analytical model and performed calculations of the temperature in the contact zone of the tool during friction-stir processing of AISI 420 steel, depending on the thermal properties of the materials and technological parameters. It is shown that feed rate reduction from 100 mm/min to 50 mm/min increases the maximum temperature in the contact zone of the rotating tool from 1250 to 1430 °C and extends holding time at the austenization temperature from 7.5 to 32.3 sec. The experimental studies of the process indirectly confirm the results of modeling based on the thickness of the hardened layer. It is shown that when the feed rate decreases from 100 mm/min to 50 mm/min, the thickness of the hardened layer increases from 850 microns to 1500 microns.

INTRODUCTION

Friction-stir processing (FSP) is an effective thermomechanical method for hardening the surface layer of steels due to intense frictional heat generation in tool/surface contact and a high degree of shear deformation. Earlier, for martensitic corrosion–resistant AISI 420 steel, it was shown that when using a WC-Co carbide tool with a flat end, the FSP implements a set of mechanisms for surface hardening by friction hardening, dynamic recrystallization, and dispersion hardening by tungsten carbide particles of the tool material. As a result of FSP, a pronounced gradient of properties is formed along the depth of the surface layer and an increase in microhardness and wear resistance is observed [1].

Classical FSP studies focus on the influence of kinematic parameters, normal force and geometry of the working part of the tool on the thermal balance and the course of dynamic recrystallization (DRX), which determines the grain size in the stir zone (SZ) and the depth of the thermomechanical affected zone (TMAZ) [2]. In FSP of steels, the geometry of the tool working part and the area of the contact zone directly affect the heat fluxes into the surface layer and the tool, which determine the development of hardening mechanisms [3].

For martensitic stainless steels of the AISI 420 type, a reduction in feed at a fixed normal force and rotation speed of the tool leads to greater heating, grain size refinement and an increase in surface microhardness. At the same time, its corrosion resistance is improved due to redistribution and refinement of the carbide phase [4]. Modern studies confirm an increase in wear resistance and a decrease in the friction coefficient of AISI 420 steel after FSP. The achieved effect is attributed to the combined contribution of dispersion hardening, as well as to the formation of compressive residual stresses [5].

FSP of structural steels provides for rapid surface hardening and improved tribological properties. Optimal processing conditions aims at achieving hardness in the stir zone, which is comparable to or exceeds the hardness after traditional quenching, and the wear of the hardened surface during dry friction is significantly reduced [6, 7]. The contact temperature is a key factor determining the surface hardening mechanism and imposing requirements on the tool material, especially on the hard alloy (Co/Ni) matrix. When overheating, the matrix softens, which leads to

tungsten carbide particles chipping and their transfer to the surface under treatment, especially when hardening high-carbon steels. [8].

Thus, for structural steels, it is necessary to make a correct choice of FSP modes, ensuring, firstly, sufficient heat supply for upper layer austenization while maintaining durability of the WC-Co tool, secondly, intensive and stable surface material stirring to minimize defects and pores, thirdly, controlled maintenance of a hardness gradient to a depth of 0.5-1.5 mm or more. The series of FSP results for AISI 420 steel with WC–Co components alloying confirms that the highest hardening effect is achieved under conditions that simultaneously provide the DRX mechanism, martensitic transformation during cooling and formation of dispersion carbide phases based on Fe–W–C.

The purpose of the work is to establish the effect of the rotating tool feed rate in the AISI 420 steel FSP on surface layer hardening due to martensitic structure formation and alloying with tungsten carbide particles based on application of the analytical model and experimental research.

MODELING AND EXPERIMENTAL RESEARCH

The friction stir processing by a tool with a spherical working part is characterized by the following main technological parameters: normal force F_n, feed rate f, rotation speed n and tool sharpening radius R_c (Fig. 1, a). Due to the normal force and heating of the material under treatment during processing, the tool is immersed to a certain depth h into the surface layer. In this case, the tool provides intensive stirring of the material under treatment up to this depth. In addition to stirring, significant heating of the material under treatment is also provided due to the frictional interaction of the tool with the material under treatment. This interaction is characterized by the frictional heat release power P_μ in the contact zone, which can be determined by the following dependence:

$$P_\mu = 2\pi F_n n R_c. \tag{1}$$

The released heat is distributed between the tool and the material under treatment into heat fluxes φ_t and φ_m, respectively (Fig. 1, b). The values of heat fluxes φ_t and φ_m are determined mainly by the thermal characteristics of the tool and materials under treatment.
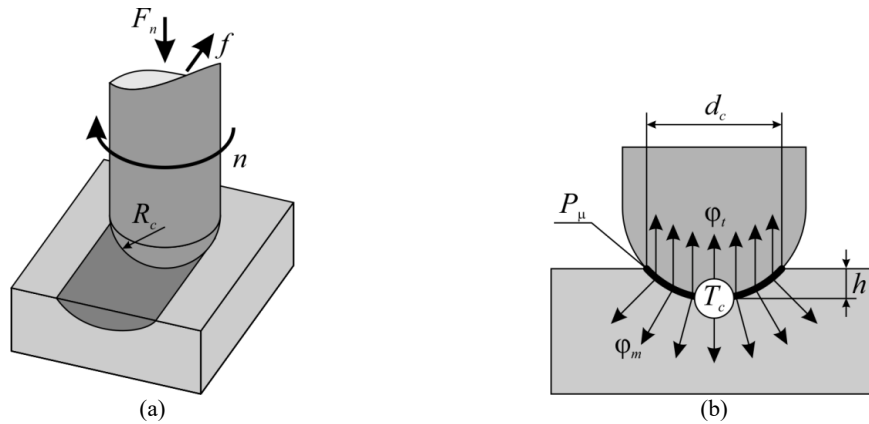

| (a) | (b) |

FIGURE 1. Scheme of friction stir processing (a) and distribution of heat fluxes (b) into the workpiece and tool

From the point of view of the reinforced surface structure formation, an important parameter is the magnitude of the heat flux φ_m entering the material under treatment and leading to its heating. The temperature T_c of the material under treatment in the tool contact zone and in the depth of the surface layer over time t can be determined using an analytical model of the semi-infinite thermal problem of a fast-moving heat source [9]:

$$T_c\left(h,t\right)=\begin{cases}\dfrac{2q_m\sqrt{at}}{\lambda}\,ierfc\left(\dfrac{h}{2\sqrt{at}}\right),\text{ when }0\le t\le t_c,\\[4mm]\dfrac{q_m}{\lambda}\left(\sqrt{at}\,ierfc\left[\dfrac{h}{2\sqrt{at}}\right]-\sqrt{a\left(t-t_c\right)}ierfc\left[\dfrac{h}{2\sqrt{a\left(t-t_c\right)}}\right]\right),\text{ when }t>t_c,\end{cases} \tag{2}$$

where q_m is the heat flux density, W/m^2; λ and α are the coefficients of thermal conductivity and temperature conductivity of the material under treatment, respectively; *ierfc* is a standard function of the multiple error function integral; t_c is the heating time during the contact of the material under treatment and the tool.

The analytical model describes the heating of the material under treatment in the contact zone over a time period of $0 \leq t \leq t_c$ and subsequent cooling after further tool travel ($t > t_c$).

The heat flux density in the material under treatment q_m can be defined as the ratio of the heat flux magnitude q_m to the contact area A_c:

$$q_m = \frac{\varphi_m}{A_c} = \frac{\varphi_m}{2\pi R_c h}. \tag{3}$$

The contact time t_c corresponds to the heating duration and can be defined as the ratio of the actual diameter of the contact spot of the tool d_c with the surface under treatment to the feed value f (4).

$$t_c = \frac{d_c}{f}. \tag{4}$$

For optimal conditions for FSP the AISI 420 steel surface with a normal force of 3000 N and a rotation speed of 2500 rpm, the dependences have been obtained that show a significant effect of the tool feed on heating and cooling of the material surface under treatment (Fig. 2). Thus, with a feed of 100 mm/min, the surface under treatment is at the temperature above the threshold A_{C3} in during 7.5 seconds, while when the feed is reduced to 75 mm/min and 50 mm/min, the austenization temperature is maintained for 15.4 and 32.3 seconds, respectively. From the findings, it can be assumed that the feed rate of 100 mm/min may be too high and will not ensure complete austenization of the surface layer material and, accordingly, the subsequent formation of a martensitic structure during cooling.
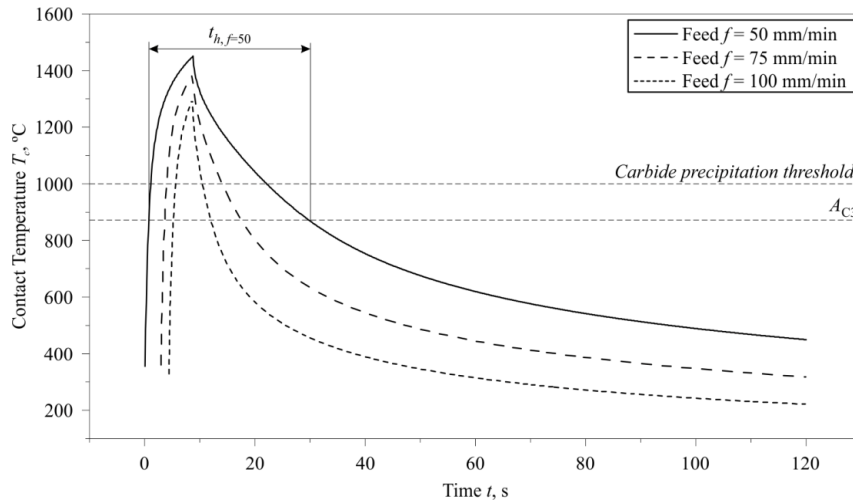

FIGURE 2. Analytical dependences of heating and cooling of the material under treatment in the tool contact zone during FSP at various tool feeds

As part of an experimental study of the process, the surface of AISI 420 steel of as-delivered condition (150 HB) was treated with a tungsten carbide tool with a cobalt binder using the modes similar to the modelling (normal force 3000 N, rotation speed 2500 rpm and feed rate of 50, 75 and 100 mm/min) (Fig. 3).
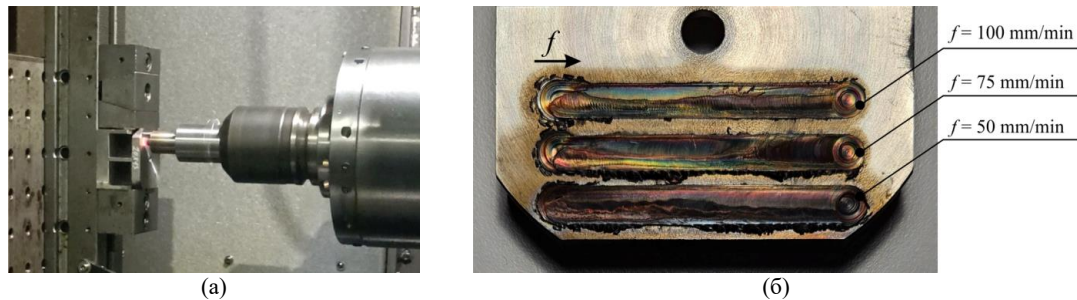
(a)	(б)

FIGURE 3. Photos of FSP at the OKUMA MA-600 processing center (a) and the friction tracks on the sample surface at feeds of 50, 75 and 100 mm/min (b)

The microstructural analysis of the friction tracks in the cross-section of the sample showed that the localized bands of alloying by the tool material particles occur in the material under treatment in the stirring zone. The erosion of the tool material into the surface layer occurs as a result of high frictional and thermal load (Fig. 4).
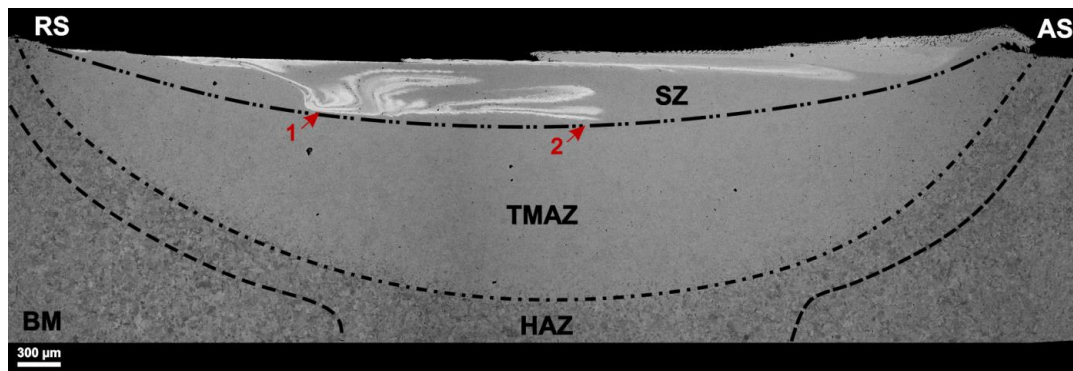

FIGURE 4. Scanning electron microscopy of the AISI 420 steel surface layer cross-section after FSP at a flow rate of 50 mm/min: SZ – stir zone; TMAZ – thermomechanically affected zone; HAZ – heat-affected zone; BM – based metal; AS – advancing side; RS – retreating side

The comparison of the cross-sections shows that the depth of the stir and thermomechanically affected zones increases with a decrease in the feed rate of the tool. At a feed rate of 50 mm/min, the depth of the SZ is 530 ± 5 microns, and the depth of the TMAZ is 1420 ± 10 microns. For samples processed at feeds of 75 mm/min and 100 mm/min, the depth of the SZ is 470 and 420 ± 5 microns, and the depth of the TMAZ is 1180 and 1080 ± 10 microns, respectively.

The analysis of the particle distribution of the tool material in the cross section under the friction track shows that during friction stirring, the highest concentration of tool material particles is located closer to the retreating side RS (Fig. 4, arrow 1). Further, as a result of the rotation and tool travel, the particles are redistributed to the advancing side, with alloying bands being formed (Fig. 4, arrow 2). In the stir zone, the areas with different tool material particle contents are formed, different in structural and phase composition, besides, the defects in the form of small pores are observed. A needle-like martensitic structure (α-Fe) with inclusions of globular grains of austenite (γ-Fe) and tungsten carbides WC is formed in a thin surface layer up to 10 microns thick after treatment with a feed rate of 50 mm/min. At the same time, in the areas with a tungsten content of 9 wt.% or more granule morphology (PRZ) prevails, whereas a needle-like martensitic structure (α'-Fe(W) and α'-Fe), respectively, is formed in the areas with a low tungsten content and with the initial level of alloying.

The results of the quantitative elemental analysis of a thin surface layer under the friction track formed during tool travels with a feed rate of 50 mm/min show the presence of inhomogeneities in saturation of the surface under treatment with tungsten carbide particles (Table 1). Based on the analysis of compositional contrast in SEM images, it is possible to identify tungsten carbide particles that appear as the brightest objects of a circumpherical shape with the size range from 0.1 to 1.5 microns. The average particle size in a thin surface layer at FSP with a feed rate of 50 mm/min was 170 nm.

TABLE 1. Summarized results of the quantitative elemental analysis of the surface layer after FSP at a feed rate of 50 mm/min

Elements	Content, wt. %						
	Spectrum 1	Spectrum 2	Spectrum 3	Spectrum 4	Spectrum 5	Dot 1	Dot 2
Cr	11.06	12.26	11.30	11.22	13.15	7.92	9.16
Fe	75.64	80.82	77.84	77.63	84.05	29.91	43.87
W	11.07	6.93	10.86	11.15	2.80	55.48	44.74
Co	2.22	0.00	0.00	0.00	0.00	3.69	2.24

In addition, the image shown in Fig. 5, a shows some lighter areas with a high content of tungsten up to 11 wt.% (Spectrum 1, 3 and 4), indicating the diffusional dissolution of the tool material in the AISI 420 steel matrix, and darker areas with low alloying up to 3 wt.% (Spectrum 2, 5). The point elemental analysis of the largest particles of the tool material WC-Co (Fig. 5, b) showed a result corresponding to the chemical composition of the tungsten carbide tool, the increased iron content is due to the fact that the analysis area exceeds the size of the particles under study.
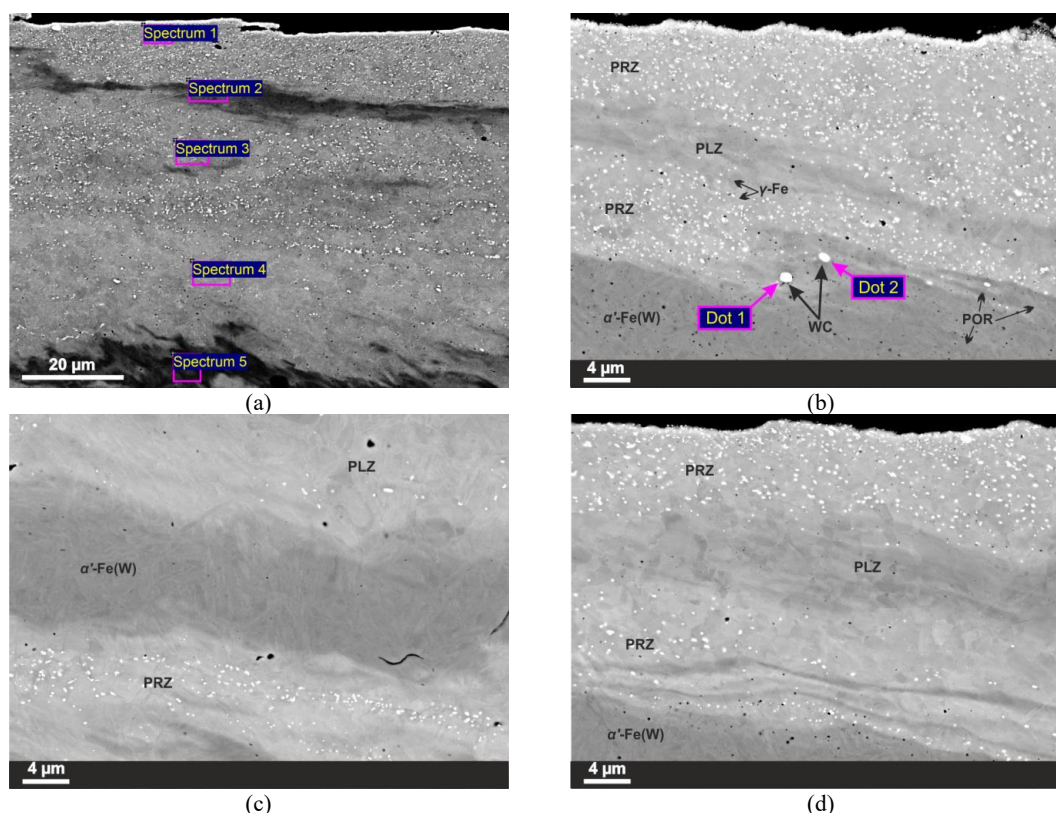

FIGURE 5. Scanning electron microscopy of a thin surface layer of a friction track after FSP at a feed rate of 50 mm/min: a – quantitative elemental analysis; b – point elemental analysis; c and d – areas of different microstructural state
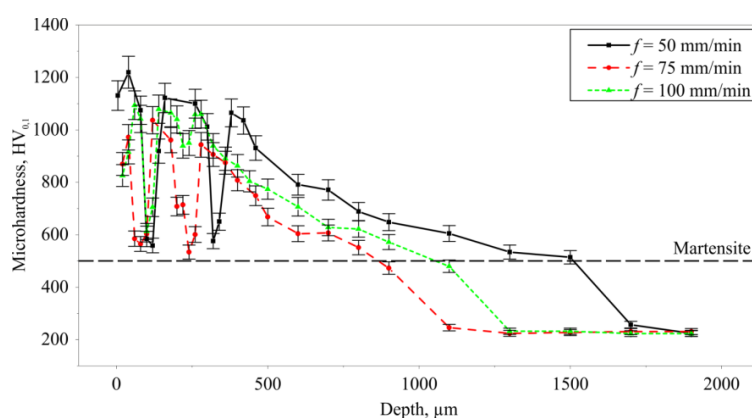
FIGURE 6. Microhardness characteristics according to the friction track depth at various feed rates

The results of microduremetry in the depth of the surface layer in the middle of the friction tracks show a similar hardening pattern of the material under treatment with a change in feed from 50 to 100 mm/min (Fig. 6). Thus, at a depth of up to 400 microns, banded hardening is observed due to the heterogeneity of alloying. Then, the microhardness gradually decreases to the initial level of ~200 $HV_{0.1}$.

CONCLUSION

The results of the experimental study are in good agreement with the temperature characteristics obtained using the analytical model. It can be seen from the microhardness characteristics that the thickness of the hardened layer increases significantly with a decrease in feed, especially to a level of 50 mm/min. Apparently, this is due to two main factors. Firstly, when the feed rate decreases, the maximum temperature in the contact area increases. Secondly, and probably more important, the exposure time of the material at high temperatures is significantly increased, which undoubtedly contributes to both more complete austenization of the material and deeper heating of the surface under treatment.

ACKNOWLEDGMENTS

REFERENCES

1. V.P. Kuznetsov, I.A.Vorontsov, M.S. Karabanalov, M.S. Khadyev, V.V. Voropaev, I.S. Kamantsev and V.P. Shveykin, Regularities of surface haedening of X20Cr13 steel by alloying with WC-Co tool material during friction stir processing. Metallovedenie i termicheskaya obrabotka metallov, **3**(387), 50–56 (2025). https://doi.org/10.30906/mitom.2025.3.50-56
2. R.S. Mishra and Z.Y. Ma, Friction stir welding and processing. Materials Science and Engineering: R: Reports **50**(1), 1–78 (2005). https://doi.org/10.1016/j.mser.2005.07.001
3. Y. Takada and H. Sasahara, Effect of Tip Shape of Frictional Stir Burnishing Tool on Processed Layer's Hardness, Residual Stress and Surface Roughness. Coatings **8**(1), 32 (2018). https://doi.org/10.3390/coatings8010032
4. L. Pan, C.T. Kwok and K.H. Lo, Enhancement in hardness and corrosion resistance of AISI 420 martensitic stainless steel via friction stir processing. Surface and Coatings Technology **357**, 339–347 (2019). https://doi.org/10.1016/j.surfcoat.2018.10.023
5. S.H. Aldajah, O.O. Ajayi, G.R. Fenske and S. David, Effect of friction stir processing on the tribological performance of high carbon steel. Wear **267**(1), 350–355 (2009). https://doi.org/10.1016/j.wear.2008.12.020
6. C. Lorenzo-Martin and O.O. Ajayi, Rapid surface hardening and enhanced tribological performance of 4140 steel by friction stir processing. Wear **332–333**, 962–970 (2015). https://doi.org/10.1016/j.wear.2015.01.052

7. S.H. Aldajah, O.O. Ajayi, G.R. Fenske and S. David, Effect of friction stir processing on the tribological performance of high carbon steel. Wear **267**(1), 350–355 (2009). https://doi.org/10.1016/j.wear.2008.12.020
8. B. Vicharapu, H. Liu, Y. Morisada, H. Fujii and A. De, Degradation of nickel-bonded tungsten carbide tools in friction stir welding of high carbon steel. Int. J. Adv. Manuf. Technol. **115**(4), 1049–1061 (2021). https://doi.org/10.1007/s00170-021-07159-3
9. J.C. Jaeger, Moving sources of heat and the temperature at sliding contacts. Journal and Proceedings of the Royal Society of New South Wales **76**(3), 203–224 (1943). https://doi.org/10.5962/p.360338